
ENHANCED BAYESIAN OPTIMIZATION VIA PREFERENTIAL MODELING OF ABSTRACT PROPERTIES

Arun Kumar A V*, Alistair Shilton, Sunil Gupta, Santu Rana, Stewart Greenhill, Svetha Venkatesh
Applied Artificial Intelligence Institute (A²I²)
Deakin University, Australia

ABSTRACT

Experimental (design) optimization is a key driver in designing and discovering new products and processes. Bayesian Optimization (BO) is an effective tool for optimizing expensive and black-box experimental design processes. While Bayesian optimization is a principled data-driven approach to experimental optimization, it learns everything from scratch and could greatly benefit from the expertise of its human (domain) experts who often reason about systems at different abstraction levels using physical properties that are not necessarily directly measured (or measurable). In this paper, we propose a human-AI collaborative Bayesian framework to incorporate expert preferences about unmeasured abstract properties into the surrogate modeling to further boost the performance of BO. We provide an efficient strategy that can also handle any incorrect/misleading expert bias in preferential judgments. We discuss the convergence behavior of our proposed framework. Our experimental results involving synthetic functions and real-world datasets show the superiority of our method against the baselines.

Keywords Machine Learning · Bayesian Optimization · Gaussian Process · Human Expert · Preferential Modeling

1 Introduction

Experimental design is the workhorse of scientific design and discovery. Bayesian Optimization (BO) has emerged as a powerful methodology for experimental design tasks Martinez-Cantin [2014], Greenhill et al. [2020] due to its sample-efficiency in optimizing expensive black-box functions. In its basic form, BO starts with a set of randomly initialized designs and then sequentially suggests the next design until the target objective is reached or the optimization budget is depleted. Theoretical analyses Srinivas et al. [2012], Chowdhury and Gopalan [2017a] of BO methods have provided mathematical guarantees of sample efficiency in the form of sub-linear regret bounds. While BO is an efficient optimization method, it only uses data gathered during the design optimization process. However, in real world experimental design tasks, we also have access to human experts Swersky [2017] who have enormous knowledge about the underlying physical phenomena. Incorporating such valuable knowledge can greatly accelerate the sample-efficiency of BO.

Previous efforts in BO literature have incorporated expert knowledge on the shape of functions Venkatesh et al. [2019], form of trends Li et al. [2018], priors over optima Hvarfner et al. [2022] and model selection Venkatesh et al. [2022], which require experts to provide very detailed knowledge about the black-box function. However, most experts understand the process in an approximate or qualitative way, and usually reason in terms of the intermediate abstract properties - the expert will compare designs, and reason as to why one design is better than another using high level abstractions. E.g, consider the design of a spacecraft shield (Whipple shield) consisting of 2 plates separated by a gap to safeguard the spacecraft against micro-meteoroid and orbital debris particle impacts. The design efficacy is measured by observing the penetration caused by hyper-velocity debris. An expert would reason why one design is better than another and accordingly come up with a new design to try out. As part of their domain knowledge, human experts often expect the first plate to shatter the space debris while the second to absorb the fragments effect. Based on these abstract intuitions, the expert will compare a pair of designs by examining the shield penetration images and ask: Does

*Mail Correspondence: a.anjanapuravenkatesh@deakin.edu.au

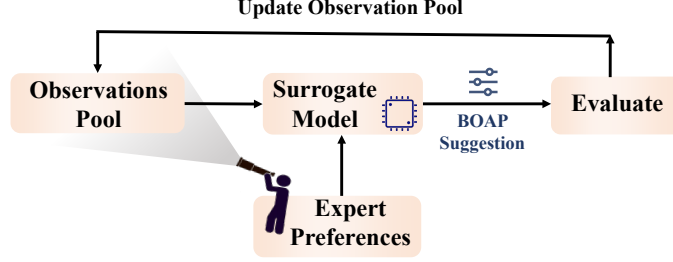


Figure 1: A schematic representation of Bayesian Optimization with Abstract Properties (BOAP)

the first plate shatter better (*Shattering*)? Does the second plate absorb the fragments better (*Absorption*)? The use of such abstractions allows experts to predict the overall design objective thus resulting in an efficient experimental design process. It is important to note that measuring such abstractions is not usually feasible and only expert’s qualitative inputs are available. *Incorporating such abstract properties in BO for the acceleration of experimental design process is not well explored.*

In this paper, we propose a novel human-AI collaborative approach - **Bayesian Optimization with Abstract Properties (BOAP)** - to accelerate BO by capturing expert inputs about the abstract, unmeasurable properties of the designs. Since expert inputs are usually qualitative Nguyen et al. [2021] and often available in the form of design preferences based on abstract properties, we model each abstract property via a latent function using the qualitative pairwise rankings. We note that eliciting such pairwise preferences about designs does not add significant cognitive overhead for the expert, in contrast to asking for explicit knowledge about properties. We fit a separate rank Gaussian process Williams and Rasmussen [2006] to model each property. Our framework allows enormous flexibility for expert collaborations as it does not need the exact value of an abstract property, just its ranking. A schematic of our proposed BOAP framework is shown in Figure 1.

Although we anticipate that experts will provide accurate preferences on abstract properties, the expert preferential knowledge can sometimes be misleading. Therefore to avoid such undesired bias, we use two models for the black-box function. The first model uses a “main” Gaussian Process (GP) to model the black-box function in an augmented input space where the design variables are augmented with the estimated abstract properties modeled via their respective rank GPs. The second model uses another “main” GP to model the black-box function using the original design space *without* any expert inputs. At each iteration, we use predictive likelihood-based model selection to choose the “best” model that has higher probability of finding the optima.

Our contributions are: (i) we propose a novel human-AI collaborative BO algorithm (BOAP) for incorporating the expert pairwise preferences on abstract properties via rank GPs (Section 3), (ii) we provide a theoretical discussion on the convergence behavior of our proposed BOAP method (Section 4), (iii) we provide empirical results on both synthetic optimization problems and real-world design optimization problems to prove the usefulness of BOAP framework (Section 5).

2 Background

2.1 Bayesian Optimization

Bayesian Optimization (BO) Brochu et al. [2010], Frazier [2018] provides an elegant framework for finding the global optima of an expensive black-box function $f(\mathbf{x})$, given as $\mathbf{x}^* \in \operatorname{argmax}_{\mathbf{x} \in \mathcal{X}} f(\mathbf{x})$, where \mathcal{X} is a compact search space. BO is comprised of two main components: (i) a surrogate model (usually a Gaussian Process Williams and Rasmussen [2006]) of the unknown objective function $f(\mathbf{x})$, and (ii) an Acquisition Function $u(\mathbf{x})$ Kushner [1964] to guide the search for optima.

2.1.1 Gaussian Process

A GP Williams and Rasmussen [2006] is a flexible, non-parametric distribution over functions. It is a preferred surrogate model because of its simplicity and tractability, in contrast to other surrogate models such as Student-t process Shah et al. [2014] and Wiener process Zhang et al. [2018]. A GP is defined by a prior mean function $\mu(\mathbf{x})$ and a kernel $k : \mathcal{X} \times \mathcal{X} \rightarrow \mathbb{R}$. The function $f(\mathbf{x})$ is modeled using a GP as $f(\mathbf{x}) \sim \mathcal{GP}(0, k(\mathbf{x}, \mathbf{x}'))$. If $\mathcal{D}_{1:t} = \{\mathbf{x}_{1:t}, \mathbf{y}_{1:t}\}$ denotes a set of observations, where $y = f(\mathbf{x}) + \eta$ is the observation corrupted with noise $\eta \in \mathcal{N}(0, \sigma_\eta^2)$ then, according to the

properties of GP, the observed samples $\mathcal{D}_{1:t}$ and a new observation $(\mathbf{x}_*, f(\mathbf{x}_*))$ are jointly Gaussian. Thus, the posterior distribution $f(\mathbf{x}_*)$ is $\mathcal{N}(\mu(\mathbf{x}_*), \sigma^2(\mathbf{x}_*))$, where $\mu(\mathbf{x}_*) = \mathbf{k}^\top [\mathbf{K} + \sigma_\eta^2 \mathbf{I}]^{-1} \mathbf{y}_{1:t}$, $\sigma^2(\mathbf{x}_*) = k(\mathbf{x}_*, \mathbf{x}_*) - \mathbf{k}^\top [\mathbf{K} + \sigma_\eta^2 \mathbf{I}]^{-1} \mathbf{k}$, $\mathbf{k} = [k(\mathbf{x}_*, \mathbf{x}_1) \cdots k(\mathbf{x}_*, \mathbf{x}_t)]^\top$, and $\mathbf{K} = [k(\mathbf{x}_i, \mathbf{x}_j)]_{i,j \in \mathbb{N}_t}$.

2.1.2 Acquisition Functions

The acquisition function selects the next point for evaluation by balancing the exploitation vs exploration (i.e searching in high value regions vs highly uncertain regions). Some popular acquisition functions include Expected Improvement Mockus et al. [1978], GP-UCB Srinivas et al. [2012] and Thompson sampling Thompson [1933]. A standard BO algorithm is provided in Appendix § A.2.

2.2 Rank GP Distributions

Kahneman and Tversky [2013] demonstrated that humans are better at providing qualitative comparisons than absolute magnitudes. Thus modeling latent human preferences is crucial when optimization objectives in domains such as A/B testing of web designing Siroker and Koomen [2015], recommender systems Brusilovski et al. [2007], players skill rating Herbrich et al. [2006] and many more. Chu and Ghahramani [2005] proposed a non-parametric Bayesian algorithm for learning instance or label preferences. We now discuss modeling pairwise preference relations using rank GPs.

Consider a set of n distinct training instances denoted by $X = \{\mathbf{x}_i \mid i \in \mathbb{N}_n \mid \mathbb{N}_n = \{1, 2, \dots, n\}\}$ based on which pairwise preference relations are observed. Let $P = \{(\mathbf{x} \succ \mathbf{x}') \mid \mathbf{x}, \mathbf{x}' \in X\}$ be a set of pairwise preference relations, where the notation $\mathbf{x} \succ \mathbf{x}'$ expresses the preference of instance \mathbf{x} over \mathbf{x}' . E.g., the pair $\{\mathbf{x}, \mathbf{x}'\}$ can be two different spacecraft shield designs and $\mathbf{x} \succ \mathbf{x}'$ implies that spacecraft design \mathbf{x} is preferred over \mathbf{x}' . Chu and Ghahramani [2005] assume that each training instance is associated with an unobservable latent function value $\{f(\mathbf{x})\}$ measured from an underlying hidden preference function $\tilde{f} : \mathbb{R}^d \rightarrow \mathbb{R}$, where $\mathbf{x} \succ \mathbf{x}'$ implies $\tilde{f}(\mathbf{x}) > \tilde{f}(\mathbf{x}')$. Employing an appropriate GP prior and likelihood, user preference can be modeled via rank GPs.

Preference learning has been used in BO literature González et al. [2017], Mikkola et al. [2020]. González et al. [2017] proposed Preferential BO (PBO) to model the unobserved objective function using a binary design preferential feedback. Benavoli et al. [2021] modified PBO to compute posteriors via skew GPs. Astudillo and Frazier [2020] proposed a preference learning based BO to model preferences in a multi-objective setup using multi-output GPs. All these works incorporate preferences about an unobserved objective function. However, in this paper, we use preference learning to model expert preferences about the intermediate abstract (auxiliary) properties. Our latent model learnt using such preferential data is then used as an input to model the main objective function.

3 Framework

This paper addresses the global optimization of an expensive, black-box function, *i.e* we aim to find:

$$\mathbf{x}^* \in \operatorname{argmax}_{\mathbf{x} \in \mathcal{X}} f(\mathbf{x}) \quad (1)$$

where $f : \mathcal{X} \rightarrow \mathbb{R}$ is a noisy and expensive objective function. For example, f could be a metric signifying the strength of the spacecraft design. The motivation of this research work is to model f by capturing the cognitive knowledge of experts in making preferential decisions based on the inherent non-measurable abstract properties of the possible designs. The objective here is same as that of standard BO *i.e.*, to find the optimal design (\mathbf{x}^*) that maximizes the unknown function f , but in the light of expert preferential knowledge on abstract properties. The central idea is to use preferential feedback to model and utilize the underlying higher-order properties that underpin preferential decisions about designs. We propose **Bayesian Optimization with Abstract Properties (BOAP)** for the optimization of f in the light of expert preferential inputs. First, we discuss expert knowledge about abstract properties. Next, we discuss GP modeling of f with preferential inputs, followed by a model-selection step that is capable of overcoming a futile expert bias in preferential knowledge. A complete algorithm for BOAP is presented in Algorithm 1 at the end of this section.

3.1 Expert Preferential Inputs on Abstract Properties

In numerous scenarios, domain experts reason the output of a system in terms of higher order properties $\omega_1(\mathbf{x}), \omega_2(\mathbf{x}), \dots$ of a design $\mathbf{x} \in \mathcal{X}$. However, these abstract properties are rarely measured, only being accessible via expert preferential inputs. E.g., a material scientist designing spacecraft shield can easily provide her pairwise preferences on the properties such as shattering, shock absorption, *i.e.*, “*this design absorbs shock better than that design*”, in contrast to specifying the exact measurements of shock absorption. These properties can be simple physical

properties or abstract combinations of multiple physical properties which an expert uses to reason about the output of a system. We propose to incorporate such qualitative properties accessible to the expert in the surrogate modeling of the given objective function to further accelerate the sample-efficiency of BO.

Let $\omega_{1:m}(\mathbf{x})$ be a set of m abstract properties derived from the design $\mathbf{x} \in \mathcal{X}$. For property ω_i , design \mathbf{x} is preferred over design \mathbf{x}' if $\omega_i(\mathbf{x}) > \omega_i(\mathbf{x}')$. We denote the set of preferences provided on ω_i as $P^{\omega_i} = \{(\mathbf{x} \succ \mathbf{x}') \mid \omega_i(\mathbf{x}) > \omega_i(\mathbf{x}') \mid \mathbf{x} \in \mathcal{X}\}$.

3.1.1 Rank GPs for Abstract Properties

We capture the aforementioned expert preferential data for each of the abstract properties $\omega_{1:m}$ individually using m separate rank Gaussian process distributions Chu and Ghahramani [2005]. In conventional GPs the observation model consists of a map of input-output pairs. In contrast, the observation model of rank (preferential) Gaussian Process (\mathcal{GP}) consists of a set of instances and a set of pairwise preferences between those instances. The central idea here is to capture the ordering over instances $X = \{\mathbf{x}_i \mid \forall i \in \mathbb{N}_n\}$ by learning latent preference functions $\{\omega_i \mid \forall i \in \mathbb{N}_m\}$. We denote such a rank GP modeling abstract property ω_i by the notation \mathcal{GP}_{ω_i} .

Let $\mathcal{X} \in \mathbb{R}^d$ be a d -dimensional compact search space and $X = \{\mathbf{x}_i \mid \forall i \in \mathbb{N}_n\}$ be a set of n training instances. Let $\omega = \{\omega(\mathbf{x})\}$ be the unobservable latent preference function values associated with each of the instances $\mathbf{x} \in X$. Let P be the set of p pairwise preferences between instances in X , defined as $P = \{(\mathbf{x} \succ \mathbf{x}')_j \mid \omega(\mathbf{x}) > \omega(\mathbf{x}') \mid \mathbf{x} \in X, \forall j \in \mathbb{N}_p\}$, where ω is the latent preference function. The observation model for the rank GP distribution \mathcal{GP}_{ω} modeling the latent preference function ω is given as $\bar{\mathcal{D}} = \{\mathbf{x}_{1:n}, P = \{(\mathbf{x} \succ \mathbf{x}')_j \mid \forall \mathbf{x}, \mathbf{x}' \in X, j \in \mathbb{N}_p\}\}$.

We follow the probabilistic kernel approach for preference learning Chu and Ghahramani [2005] to formulate the likelihood function and Bayesian probabilities. Imposing non-parametric GP priors on the latent function values ω , we arrive at the prior probability of ω given by:

$$\mathcal{P}(\omega) = (2\pi)^{-\frac{n}{2}} |\mathbf{K}|^{-\frac{1}{2}} \exp\left(-\frac{1}{2} \omega^\top \mathbf{K}^{-1} \omega\right) \quad (2)$$

With suitable noise assumptions $\mathcal{N}(0, \tilde{\sigma}_\eta^2)$ on inputs and the preference relations $(\mathbf{x}, \mathbf{x}')_{1:m}$ in P , the Gaussian likelihood function based on Thurstone [2017] is:

$$\mathcal{P}((\mathbf{x} \succ \mathbf{x}')_i \mid \omega(\mathbf{x}), \omega(\mathbf{x}')) = \Phi(z_i(\mathbf{x}, \mathbf{x}')) \quad (3)$$

where Φ is the c.d.f of standard normal distribution $\mathcal{N}(0, 1)$ and $z(\mathbf{x}, \mathbf{x}') = \frac{\omega(\mathbf{x}) - \omega(\mathbf{x}')}{\sqrt{2\tilde{\sigma}_\eta^2}}$. Based on Bayes theorem, the posterior distribution of the latent function given the data is given by:

$$\mathcal{P}(\omega \mid \bar{\mathcal{D}}) = \frac{\mathcal{P}(\omega)}{\mathcal{P}(\bar{\mathcal{D}})} \mathcal{P}(\bar{\mathcal{D}} \mid \omega)$$

where $\mathcal{P}(\omega)$ is the prior distribution (Eq. (2)), $\mathcal{P}(\bar{\mathcal{D}} \mid \omega)$ is the probability of observing the pairwise preferences given the latent function values ω , which can be computed as a product of the likelihood (Eq. (3)) i.e., $\mathcal{P}(\bar{\mathcal{D}} \mid \omega) = \prod_p \mathcal{P}((\mathbf{x} \succ \mathbf{x}')_p \mid \omega(\mathbf{x}), \omega(\mathbf{x}'))$ and $\mathcal{P}(\bar{\mathcal{D}}) = \int \mathcal{P}(\bar{\mathcal{D}} \mid \omega) \mathcal{P}(\omega) d\omega$ is the evidence of model parameters including kernel hyperparameters. We find the posterior distribution using Laplace approximation and the Maximum A Posteriori estimate (MAP) ω_{MAP} as the mode of posterior distribution. We can find the MAP using Newton-Raphson descent given by:

$$\omega^{\text{new}} = \omega^{\text{old}} - \mathbf{H}^{-1} \mathbf{g} \mid_{\omega=\omega^{\text{old}}} \quad (4)$$

where the Hessian $\mathbf{H} = [\mathbf{K} + \tilde{\sigma}_\eta^2 \mathbf{I}]^{-1} + \mathbf{C}$, and the gradient $\mathbf{g} = \nabla_\omega \log \mathcal{P}(\omega \mid \bar{\mathcal{D}}) = -[\mathbf{K} + \tilde{\sigma}_\eta^2 \mathbf{I}]^{-1} \omega + \mathbf{b}$, given $b_j = \frac{\partial}{\partial \omega(\mathbf{x}_j)} \sum_p \ln \Phi(z_p)$ and $C_{ij} = \frac{\partial}{\partial \omega(\mathbf{x}_i) \partial \omega(\mathbf{x}_j)} \sum_p \ln \Phi(z_p)$.

3.1.2 Hyperparameter Optimization

Kernel hyperparameter (θ^*) is crucial to optimize the generalization performance of the GP. We perform the model selection for our rank-GPs by maximizing the corresponding log-likelihood in the light of latent values ω_{MAP} . In contrast to the evidence maximization mentioned in Chu and Ghahramani [2005] i.e., $\theta^* = \arg\max_\theta \mathcal{P}(\bar{\mathcal{D}} \mid \theta)$, we find the optimal kernel hyperparameters by maximizing the log-likelihood ($\bar{\mathcal{L}}$) of rank GPs i.e., $\theta^* = \arg\max_\theta \bar{\mathcal{L}}$. The closed-form of log-likelihood of the rank GP is given as:

$$\bar{\mathcal{L}} = -\frac{1}{2} \omega_{\text{MAP}}^\top [\mathbf{K} + \tilde{\sigma}_\eta^2 \mathbf{I}]^{-1} \omega_{\text{MAP}} - \frac{1}{2} \log |\mathbf{K} + \tilde{\sigma}_\eta^2 \mathbf{I}| - \frac{n}{2} \log(2\pi) \quad (5)$$

3.2 Augmented GP with Abstract Property Preferences

To account for property preferences in modeling f , we augment the input \mathbf{x} of a conventional GP modeling f with the mean predictions obtained from m rank GPs ($\mathcal{GP}_{\omega_{1:m}}$) as auxiliary inputs capturing the property preferences $\omega_{1:m}$, *i.e.*, instead of modeling GP directly on \mathbf{x} we model on $\tilde{\mathbf{x}} = [\mathbf{x}, \mu_{\omega_1}(\mathbf{x}), \dots, \mu_{\omega_m}(\mathbf{x})]$, where μ_{ω_i} is the predictive mean computed using:

$$\mu_{\omega_i}(\mathbf{x}) = \mathbf{k}^\top [\mathbf{K} + \sigma_\eta^2 \mathbf{I}]^{-1} \boldsymbol{\omega}_{\text{MAP}}$$

where $\mathbf{k} = [k(\mathbf{x}, \mathbf{x}_1), \dots, k(\mathbf{x}, \mathbf{x}_n)]^\top$, $\mathbf{K} = [k(\mathbf{x}_i, \mathbf{x}_j)]_{i,j \in \mathbb{N}_n}$ and $\mathbf{x}_i \in X$. To handle different scaling levels in rank GPs, we normalize its output in the interval $[0, 1]$, such that $\mu_{\omega_i}(\mathbf{x}) \in [0, 1]$.

Although we model $\tilde{\mathbf{x}}$ using mean predictions $\mu_{\omega_i}(\mathbf{x})$, the uncertainty estimates were not (directly) considered in the modeling. The GP predictive variance tends to be high outside of the neighborhood of observations, indicating the uncertainty in our beliefs on the model. Therefore, a data point with high predictive variance $(\sigma_{\omega_1}(\mathbf{x}))^2$ in rank GP indicate the model uncertainty. We incorporate this uncertainty in our main GP modeling $\tilde{\mathbf{x}}$ such that the effects of predicted abstract properties $\mu_{\omega_i}(\mathbf{x})$ are appropriately reduced when the model is uncertain *i.e.* when $(\sigma_{\omega_i}(\mathbf{x}))^2$ is high.

To achieve this, we formulate the feature-wise lengthscales as a function of predictive uncertainty of the augmented dimensions to control their *importance* in the overall GP. Note that augmented features can be detrimental when the model is uncertain. To address this potential problem, we use a spatially varying kernel Venkatesh et al. [2019] that treats the lengthscale as a function of the input, rather than a constant. A positive definite kernel with spatially varying lengthscale is given as:

$$k(\mathbf{x}, \mathbf{x}') = \prod_{d=1}^D \sqrt{\frac{2l(x_d)l(x'_d)}{l^2(x_d) + l^2(x'_d)}} \exp \left(- \sum_{d=1}^D \frac{(x_d - x'_d)^2}{l^2(x_d) + l^2(x'_d)} \right) \quad (6)$$

where $l(\cdot)$ is the lengthscale function. In our proposed framework, we use lengthscale as a function *i.e.*, $l(\cdot)$ only for the newly augmented dimensions and set the lengthscale of the original dimensions to a constant value *i.e.* $\theta = [l_1, \dots, l_D, l_{\omega_1}(\mathbf{x}), \dots, l_{\omega_m}(\mathbf{x})]$. As we need lengthscale function to reflect the model uncertainty, we set $l_{\omega_i}(\mathbf{x}) = \alpha \tilde{\sigma}_{\omega_i}(\mathbf{x})$, where $\tilde{\sigma}_{\omega_i}(\mathbf{x})$ is the normalized standard deviation of the rank GP predicted for the abstract property ω_i and α is a scale parameter that is tuned using the standard GP log-marginal likelihood in conjunction with other kernel parameters. The aforementioned lengthscales ensure that the data points $\tilde{\mathbf{x}}$ with high model uncertainty have higher lengthscale on the augmented dimensions and thus are treated as less important.

The objective function is modeled on the concatenated inputs $\tilde{\mathbf{x}} \in \mathbb{R}^{d+m}$ and we denote this function with augmented inputs $\tilde{\mathbf{x}}$ as human-inspired objective function $h(\tilde{\mathbf{x}})$. The GP (\mathcal{GP}_h) constructed in the light of expert preferential data is then used in BO to find the global optima of $h(\tilde{\mathbf{x}})$, given as:

$$\mathbf{x}^* \in \underset{\mathbf{x} \in \mathcal{X}}{\operatorname{argmax}} h(\tilde{\mathbf{x}}) \quad (7)$$

The observation model is $\mathcal{D} = \{(\mathbf{x}, y = h(\tilde{\mathbf{x}}) \approx f(\mathbf{x}))\}$ *i.e.*, the human-inspired objective function $h(\tilde{\mathbf{x}})$ is a simplified $f(\mathbf{x})$ with auxiliary features in the input, thus we observe the $h(\tilde{\mathbf{x}})$ via $f(\mathbf{x})$.

3.3 Overcoming Inaccurate Expert Inputs

Up to this point we have assumed that expert input is accurate and thus likely to accelerate BO. However, in some cases this feedback may be inaccurate, and potentially slowing optimization. To overcome such bias and encourage exploration we maintain 2 models, one of which is augmented by expert abstract properties (we refer to this as Human Arm-h) and an un-augmented model (we refer to this as Control Arm-f), and use predictive likelihood to select the arm at each iteration.

The experimental arm models f directly by observing the function values at suggested candidate points. Here, we fit a standard GP (\mathcal{GP}_f) based on the data collected *i.e.*, $\mathcal{D} = \{(\mathbf{x}, y = f(\mathbf{x}) + \eta)\}$ where $\eta \sim \mathcal{N}(0, \sigma_\eta^2)$ is the Gaussian noise. The GP distribution (\mathcal{GP}_f) may be used to optimize f using a BO algorithm with Thompson Sampling (TS) Thompson [1933] strategy.

At each iteration t , we compare the predictive likelihoods (\mathcal{L}_t) of both the human augmented arm (Arm-h) and an experimental arm (Arm-f) to select the arm to pull for suggesting the next promising candidate for the function evaluation. Then, we use Thompson sampling to draw a sample S_t from the GP posterior distribution of the arm pulled and find its corresponding maxima given as:

$$\mathbf{x}_t^h = \operatorname{argmax}_{\mathbf{x} \in \mathcal{X}} (S^h(\tilde{\mathbf{x}})); \quad \mathbf{x}_t^f = \operatorname{argmax}_{\mathbf{x} \in \mathcal{X}} (S^f(\mathbf{x}))$$

The arm with maximum predictive likelihood is chosen at each iteration and we observe f at the suggested location *i.e.*, $(\mathbf{x}_t^h, f(\mathbf{x}_t^h))$ or $(\mathbf{x}_t^f, f(\mathbf{x}_t^f))$. Then rank GPs are updated to capture the preferences with respect to the new suggestion \mathbf{x}_t^h or \mathbf{x}_t^f . This process continues until the evaluation budget T is exhausted. Additional details of BOAP framework is provided in the Appendix (§ A.3).

Algorithm 1 BO with Preferences on Abstract Properties (BOAP)

Input: Initial Observations: $\mathcal{D}_{1:t'} = \{\mathbf{x}_{1:t'}, \mathbf{y}_{1:t'}\}$, Preferences: $P^{\omega_i} = \{(\mathbf{x} \succ \mathbf{x}')_{1:p} \mid \forall i \in \mathbb{N}_m\}$

1. **for** $t = t' + 1, \dots, T$ iterations **do**
 2. optimize hyperparameters $\Theta_t^* = \{\theta_{\omega_{1:m}}^*, \theta_h^*, \theta_f^*\}$ and update $\mathcal{GP}_{\omega_{1:m}}, \mathcal{GP}_h, \mathcal{GP}_f$
 3. compute predictive likelihoods \mathcal{L}_t^h and \mathcal{L}_t^f for Arm-h and Arm-f
 4. **if** $\mathcal{L}_t^h > \mathcal{L}_t^f$, **then**
 5. draw a random sample S_t^h from Arm-h using Thompson Sampling
 6. maximize S_t^h to find $\mathbf{x}_t^h = \operatorname{argmax}_{\mathbf{x} \in \mathcal{X}} (S_t^h(\tilde{\mathbf{x}}))$
 7. $\mathbf{x}_t = \mathbf{x}_t^h$
 8. **else,**
 9. draw a random sample S_t^f from Arm-f using Thompson Sampling
 10. maximize S_t^f to find $\mathbf{x}_t^f = \operatorname{argmax}_{\mathbf{x} \in \mathcal{X}} (S_t^f(\mathbf{x}))$
 11. $\mathbf{x}_t = \mathbf{x}_t^f$
 12. evaluate f at \mathbf{x}_t to obtain $y_t = f(\mathbf{x}_t) + \eta_t$
 13. Augment data $\mathcal{D} = \mathcal{D} \cup (\mathbf{x}_t, y_t)$ and update expert preferences $P^{\omega_{1:m}}$ with respect to \mathbf{x}_t
 14. $\mathbf{x}^* = \operatorname{argmax}_{(\mathbf{x}, y) \in \mathcal{D}} y$
 15. **end for**
 16. **return** \mathbf{x}^*
-

4 Convergence Remarks

In this section we discuss the convergence properties of BOAP algorithm. The essence of BOAP is the combination of Thompson-Sampling Bayesian Optimization (TS-BO) with likelihood-based model-selection from multiple models of the same objective. To understand the convergence properties, we begin with special cases and then generalize to the real case.

Purely Un-Augmented Case: Let us suppose that the non-augmented (Control arm) model is used for all iterations of BOAP. In this mode of operation BOAP will operate precisely like standard Thompson-sampling BO (TS-BO), and thus regret is bounded as per TS-BO Russo and Van Roy [2014], Kandasamy et al. [2018], Chowdhury and Gopalan [2017b] - *i.e.*, in this simplified case the (cumulative) regret is bounded as $R_T \sim \mathcal{O}(\sqrt{T}(B\sqrt{\gamma_T} + \gamma_T))$ if we assume $f \in \mathcal{H}_K$ and $\|B\|_{\mathcal{H}_K} \leq B$, where γ_T is the maximum information gain (which is controlled by the covariance prior k). Alternatively, assuming $f \in \mathcal{F}$, the Bayes regret is bounded as $\text{BR}_T \sim \mathcal{O}(\sqrt{\dim_E(\mathcal{F}, \frac{1}{T})T \log T})$ Russo and Van Roy [2014], where $\dim_E(\mathcal{F}, \frac{1}{T})$ is the eluder dimension of \mathcal{F} Russo and Van Roy [2014], Li et al. [2021] as defined below (see Definition 3.2).

Definition 1 (ϵ -independence). *Russo and Van Roy [2014] Let $\mathcal{F} \subset \mathbb{R}^{\mathcal{X}}$, $\epsilon \in \mathbb{R}^+$. Then $\mathbf{x} \in \mathcal{X}$ is ϵ -dependent of $\{\mathbf{x}_1, \mathbf{x}_2, \dots, \mathbf{x}_n\} \subset \mathcal{X}$ if, $\forall f, f' \in \mathcal{F}$ such that $\sum_i (f(\mathbf{x}_i) - f'(\mathbf{x}_i))^2 \leq \epsilon^2$, then $|f(\mathbf{x}) - f'(\mathbf{x})| < \epsilon$. We say that $\mathbf{x} \in \mathcal{X}$ is ϵ -independent if it is not ϵ -dependent.*

Definition 2 (Eluder dimension). *Russo and Van Roy [2014] Let $\mathcal{F} \subset \mathbb{R}^{\mathcal{X}}$, $\epsilon \in \mathbb{R}^+$. The eluder dimension $\dim_E(\mathcal{F}, \epsilon)$ of \mathcal{F} is the length of the longest sequence $\{\mathbf{x}_1, \mathbf{x}_2, \dots, \mathbf{x}_n\} \subset \mathcal{X}$ such that $\forall i, \exists \epsilon' \geq \epsilon$ such that \mathbf{x}_i is ϵ' -independent of $\{\mathbf{x}_1, \mathbf{x}_2, \dots, \mathbf{x}_{i-1}\}$.*

Eluder Dimension is a measure of effective dimension, being the number of observations required to model any function in the set to within a given accuracy.

Purely Augmented Case: Next, suppose that the augmented model (Human Arm) is used for all iterations of BOAP. In this case the overall objective model is not a GP (due to the involvement of rank GP as an input to the main GP), so we cannot naively apply information-gain based TS-BO regret bounds as we may for the Control Arm case. However we can apply the eluder dimension bounds. Whether this provides better convergence depends entirely on the relevance and accuracy of the user expert feedback used to construct the model augmentation: accurate feedback of relevant abstract properties should, we postulate, reduce the eluder dimension of the model (with the limiting case where the augmentation models f), while inaccurate or irrelevant feedback may mislead the model and increase eluder dimension, impeding convergence.

General Case: More generally, BOAP may select between the Control and Experimental Arms, which can be modeled stochastically. If neither model has a consistently higher likelihood (either initially or asymptotically) then the convergence behaviour will follow the worst-case convergence of TS-BO using either the un-augmented or augmented model alone - that is:

$$\text{BR}_T \sim \mathcal{O}(\sqrt{\max\{\dim_E(\mathcal{F}_f, \frac{1}{T}), \dim_E(\mathcal{F}_h, \frac{1}{T})\}} T \log T)$$

Under the reasonable assumptions that the predictive likelihood is (a) an accurate measure of model fit, and that asymptotically (b) $\mathcal{L}_t^h > \mathcal{L}_t^f$ if $\dim_E(\mathcal{F}_h, \frac{1}{T}) < \dim_E(\mathcal{F}_f, \frac{1}{T})$ (and vice-versa) then:

$$\text{BR}_T \sim \mathcal{O}(\sqrt{\min\{\dim_E(\mathcal{F}_f, \frac{1}{T}), \dim_E(\mathcal{F}_h, \frac{1}{T})\}} T \log T)$$

So, provided that the expert provides accurate and relevant preference feedback we would have that (a) the augmented model will (asymptotically) be selected and thus dominate the regret bound, and (b) due to its lower eluder dimension the regret bound will be tighter, leading to a faster convergence.

5 Experiments

We evaluate the performance of BOAP method using synthetic benchmark function optimization problems and real-world optimization problems arising in advanced battery manufacturing processes. We have considered the following experimental settings for BOAP. We use the popular Automatic Relevance Determination (ARD) kernel Neal [2012] for the construction of both the rank GPs and the conventional (un-augmented) GPs. For rank GPs, we tune ARD kernel hyperparameters $\theta_d = \{l_d\}$ using max-likelihood estimation (Eq. (5)). For the augmented GP modeling $\tilde{\mathbf{x}}$, we use a modified ARD kernel that uses spatially varying kernel with a parametric lengthscale function (See discussion in § 3.2). As we normalize the bounds, we tune l_d (the lengthscale for the *un*-augmented features) in the interval $[0.1, 1]$ and the scale parameter α (for the auxiliary features) in the interval $(0, 2]$. Further, we set signal variance $\sigma_f^2 = 1$ as we standardize the outputs.

We compare the performance of BOAP algorithm with the following state-of-the-art baselines. **(i) BO-TS:** a standard Bayesian Optimization (BO) with Thompson Sampling (TS) strategy, **(ii) BO-EI:** BO with Expected Improvement (EI) acquisition function, and **(iii) BOAP - Only Augmentation (BOAP-OA):** In this baseline, we run our algorithm without the 2-arm scheme and we only use augmented input for GP modeling. This baseline shows the effectiveness of expert’s inputs.. We do not consider any preference based BO methods González et al. [2017], Benavoli et al. [2021] as baselines, because the preferences are provided directly on the objective function, as opposed to abstract properties that are not measured directly. The additional experimental results and details of our experimental setup are provided in the Appendix (§ A.4.1).

5.1 Synthetic Experiments

We evaluate BOAP framework in the global optimization of synthetic optimization benchmark functions Surjanovic and Bingham [2017]. The list of synthetic functions used are provided in Table 1.

Emulating Preferential Expert Inputs: As discussed in §3.1, we fit a rank GP using the expert preferences provided on designs based on their cognitive knowledge. In all our synthetic experiments we set $m = 2$, *i.e.*, we model two abstract properties $\{\omega_1, \omega_2\}$ for the considered synthetic function. We expect the expert to know the higher order

Table 1: Details of the synthetic optimization benchmark functions. Analytical forms are provided in the 2nd column and the last column depicts the high level features used by a simulated expert.

Functions	$f(\mathbf{x})$	High Level Features
Benchmark-1d	$\exp^{(2-\mathbf{x})^2} + \exp^{\frac{(6-\mathbf{x})^2}{10}} + \frac{1}{\mathbf{x}^2+1}$	$\omega_1 = \exp^{(2-\mathbf{x})^2}, \omega_2 = \frac{1}{\mathbf{x}^2}$
Rosenbrock-3d	$\sum_{i=1}^{d-1} [100 \times (x_{i+1} - x_i^2)^2 + (x_i - 1)^2]$	$\omega_1 = (x_3 - x_2^2)^2 + (x_2 - x_1^2)^2$ $\omega_2 = (x_2 - 1)^2 + (x_1 - 1)^2$
Griewank-5d	$\sum_{i=1}^d \left[\frac{x_i^2}{4000} - \prod_{i=1}^d \cos\left(\frac{x_i}{\sqrt{i}}\right) + 1 \right]$	$\omega_1 = \sum_{i=1}^d x_i^2, \omega_2 = \prod_{i=1}^d \cos x_i$

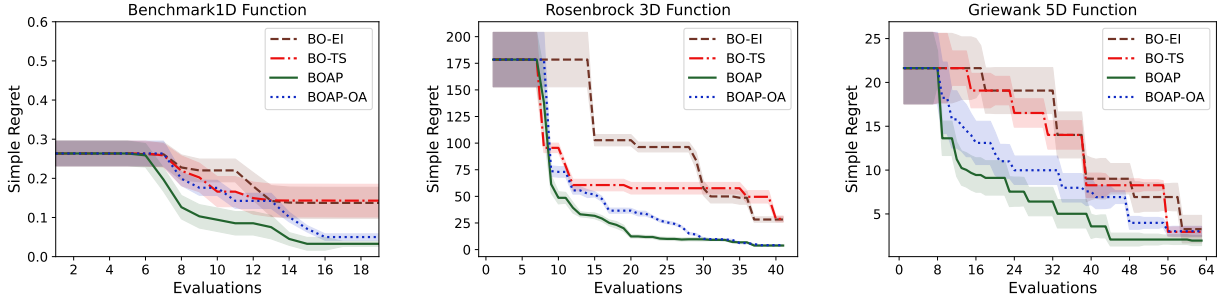


Figure 2: Simple regret vs iterations for the synthetic multi-dimensional benchmark functions. We plot the average regret along with its standard error obtained after 10 random repeated runs.

abstract features of each design $\mathbf{x} \in \mathcal{X}$. We construct rank GPs by emulating the expert preferences based on such high-level features of the given synthetic function. The possible set of high-level features of the synthetic functions are mentioned in Table 1. We generate preference list $P^{\omega_{1:2}}$ for each high-level feature of the designs by comparing its utility. We start with $p = \binom{t'}{2}$ preferences in P , that gets updated in every iteration of the optimization process. We construct rank GP surrogates $\{\mathcal{GP}_{\omega_1}, \mathcal{GP}_{\omega_2}\}$ using P^{ω_1} and P^{ω_2} .

For a given d -dimensional problem, we have considered $t' = d + 3$ initial observations and allocate the overall budget $T = 10 \times d + 5$. We repeat all our synthetic experiments 10 times with random initialization and report the average simple regret Brochu et al. [2010] as a function of iterations. The convergence plots obtained for the global optimization experiments of synthetic functions after 10 runs are shown in Figure 2. It is evident from the convergence results that our proposed BOAP method has outperformed the standard baselines by a huge margin, thereby proving its superiority.

To demonstrate the effectiveness of BOAP we have conducted additional experiments by accounting for the inaccuracy or poor choices in expert preferential knowledge. Please refer to Appendix (§ A.4) for the additional details and experimental results.

5.2 Real-world Experiments

We compare the performance of BOAP in two real-world optimization use-cases in Lithium-ion battery manufacturing that are proven to be very complex and expensive in nature, thus providing a wide scope for the optimization. Further, battery scientists often reveal additional knowledge about the abstract properties in the battery design space and thus providing a rich playground for the evaluation of our framework. We refer to the appendix (§ A.4.3) for the detailed experimental setup.

5.2.1 Optimization of Electrode Calendering

In this experiment, we consider a case study on the calendering process proposed by Duquesnoy et al. [2020]. The authors analyzed the effect of parameters such as calendering pressure (ε_{cal}), electrode porosity and electrode composition on the electrode properties such as electrolyte conductivity, tortuosity (both in solid phase (τ_{sol}) and liquid phase (τ_{liq})), Current Collector (CC), Active Surface (AS), etc. We define an optimization paradigm using the data published by Duquesnoy et al. [2020].

We use our proposed BOAP framework to optimize the electrode calendering process by maximizing the *Active Surface* of electrodes by modeling two abstract properties: (i) Property 1 (ω_1): *Tortuosity in liquid phase* τ_{liq} , and (ii) Property 2

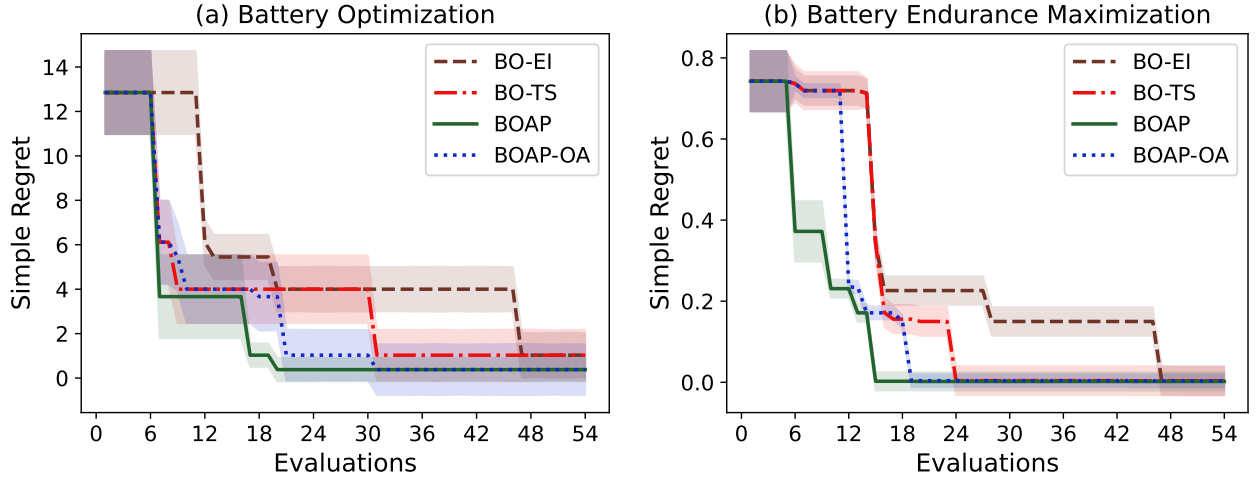


Figure 3: Simple regret vs iterations for battery manufacturing optimization experiments: **(a)** Optimization of calendaring process **(b)** Optimization of battery endurance.

(ω_2): *Output Porosity* (OP). We simulate the expert pairwise preferential inputs $\{P^{\omega_{\text{Tiq}}}, P^{\omega_{\text{OP}}}\}$ by comparing the actual measurements reported in the dataset published by Duquesnoy et al. [2020]. We consider 4 initial observations and maximize the active surface of the electrodes for 50 iterations. We compare the performance of our proposed BOAP framework by plotting the average simple regret after 10 repeated runs with random initialization. The convergence results obtained for the electrode optimization is shown in Figure 3a.

5.2.2 Electrode Manufacturing Optimization

The best battery formulation and the optimal selection of process parameters is crucial for manufacturing long-life and energy-dense batteries. Drakopoulos et al. [2021] analyzed the manufacturing of Lithium-ion graphite based electrodes and reported the process parameters in manufacturing a battery along with the output charge capacities of the battery measured after certain charge-discharge cycles. In our experiment, we use BOAP to optimally select the manufacturing process parameters to design a battery with maximum endurance *i.e.*, a battery that can retain the maximum charge after certain charge-discharge cycles. We consider *Anode Thickness* (AT) and *Active Mass* (AM) as abstract properties $\{\omega_{\text{AT}}, \omega_{\text{AM}}\}$ to maximize the battery endurance $E = \frac{D_{50}}{D_5}$, where D_{50} and D_5 are the discharge capacities of the cell at 50th and 5th cycle, respectively. We consider 4 initial observations and maximize the endurance of the cell for 50 iterations. We compare the performance by plotting the average simple regret versus iterations after 10 random repeated runs. The convergence results obtained for maximizing the endurance is shown in Figure 3b.

It is evident from Figure 3 that BOAP is superior to the baselines due to its ability to model the abstract properties of the battery designs that can be beneficial in accelerating BO performance.

6 Conclusion

We present a novel approach for human-AI collaborative BO for modeling the expert inputs on abstract properties to further accelerate the sample-efficiency of BO. Experts provide preferential inputs about the abstract and unmeasurable properties. We model such preferential inputs using rank GPs. We augment the inputs of a standard GP with the output of such auxiliary rank GPs to learn the underlying preferences in the instance space. We use a 2-arm strategy to overcome any futile expert bias and encourage exploration. We discuss the convergence of our proposed BOAP framework. The experimental results show the superiority of our proposed BOAP algorithm.

References

- Ruben Martinez-Cantin. BayesOpt: a Bayesian optimization library for nonlinear optimization, experimental design and bandits. *J. Mach. Learn. Res.*, 15(1):3735–3739, 2014.
- Stewart Greenhill, Santu Rana, Sunil Gupta, Pratibha Vellanki, and Svetha Venkatesh. Bayesian optimization for adaptive experimental design: a review. *IEEE access*, 8:13937–13948, 2020.
- Niranjan Srinivas, Andreas Krause, Sham M Kakade, and Matthias W Seeger. Information-theoretic regret bounds for Gaussian process optimization in the bandit setting. *IEEE Transactions on Information Theory*, 58(5):3250–3265, 2012.
- Sayak Ray Chowdhury and Aditya Gopalan. On kernelized multi-armed bandits. In *International Conference on Machine Learning*, pages 844–853. PMLR, 2017a.
- Kevin Swersky. *Improving Bayesian optimization for machine learning using expert priors*. University of Toronto (Canada), 2017.
- Arun Kumar Anjanapura Venkatesh, Santu Rana, Cheng Li, Sunil Gupta, Alistair Shilton, and Svetha Venkatesh. Bayesian optimization for objective functions with varying smoothness. In *Australasian Joint Conference on Artificial Intelligence*, pages 460–472, 2019.
- Cheng Li, Rana Santu, Sunil Gupta, Vu Nguyen, Svetha Venkatesh, Alessandra Sutti, David Rubin, Teo Slezak, Murray Height, Mazher Mohammed, and Ian Gibson. Accelerating experimental design by incorporating experimenter hunches. In *2018 IEEE International Conference on Data Mining (ICDM)*, pages 257–266, 2018. doi:10.1109/ICDM.2018.00041.
- Carl Hvarfner, Danny Stoll, Artur Souza, Marius Lindauer, Frank Hutter, and Luigi Nardi. π BO: Augmenting Acquisition Functions with User Beliefs for Bayesian Optimization. *arXiv preprint arXiv:2204.11051*, 2022.
- Arun Kumar Anjanapura Venkatesh, Santu Rana, Alistair Shilton, and Svetha Venkatesh. Human-AI Collaborative Bayesian optimization. In *Advances in Neural Information Processing Systems*, 2022.
- Quoc Phong Nguyen, Sebastian Tay, Bryan Kian Hsiang Low, and Patrick Jaillet. Top-k ranking Bayesian optimization. In *Proceedings of the AAAI Conference on Artificial Intelligence*, volume 35, pages 9135–9143, 2021.
- Christopher KI Williams and Carl Edward Rasmussen. *Gaussian processes for machine learning*, volume 2. MIT press Cambridge, MA, 2006.
- Eric Brochu, Vlad M Cora, and Nando De Freitas. A tutorial on Bayesian optimization of expensive cost functions, with application to active user modeling and hierarchical reinforcement learning. *arXiv preprint arXiv:1012.2599*, 2010.
- Peter I Frazier. A tutorial on Bayesian optimization. *arXiv preprint arXiv:1807.02811*, 2018.
- H. J. Kushner. A new method of locating the maximum point of an arbitrary multipeak curve in the presence of noise. *Journal of Basic Engineering*, 86(1):97–106, 03 1964. ISSN 0021-9223. doi:10.1115/1.3653121.
- Amar Shah, Andrew Wilson, and Zoubin Ghahramani. Student-t processes as alternatives to Gaussian processes. In *Artificial intelligence and statistics*, pages 877–885, 2014.
- Zhengxin Zhang, Xiaosheng Si, Changhua Hu, and Yaguo Lei. Degradation data analysis and remaining useful life estimation: A review on Wiener-process-based methods. *European Journal of Operational Research*, 271(3): 775–796, 2018.
- Jonas Mockus, Vytautas Tiesis, and Antanas Zilinskas. The application of Bayesian methods for seeking the extremum. In *Towards Global Optimization*, volume 2, pages 117–129. September 1978. ISBN 0-444-85171-2.
- William R Thompson. On the likelihood that one unknown probability exceeds another in view of the evidence of two samples. *Biometrika*, 25(3-4):285–294, 1933.
- Daniel Kahneman and Amos Tversky. Prospect theory: An analysis of decision under risk. In *Handbook of the fundamentals of financial decision making: Part I*, pages 99–127. World Scientific, 2013.
- Dan Siroker and Pete Koomen. *A/B testing: The most powerful way to turn clicks into customers*. John Wiley & Sons, 2015.
- Peter Brusilovski, Alfred Kobsa, and Wolfgang Nejdl. *The adaptive web: methods and strategies of web personalization*, volume 4321. Springer Science & Business Media, 2007.
- Ralf Herbrich, Tom Minka, and Thore Graepel. TrueSkill: a Bayesian skill rating system. *Advances in neural information processing systems*, 19, 2006.
- Wei Chu and Zoubin Ghahramani. Preference learning with Gaussian processes. In *Proceedings of the 22nd international conference on Machine learning*, pages 137–144, 2005.

- Javier González, Zhenwen Dai, Andreas Damianou, and Neil D Lawrence. Preferential bayesian optimization. In *International Conference on Machine Learning*, pages 1282–1291. PMLR, 2017.
- Petrus Mikkola, Milica Todorović, Jari Järvi, Patrick Rinke, and Samuel Kaski. Projective preferential bayesian optimization. In *International Conference on Machine Learning*, pages 6884–6892. PMLR, 2020.
- Alessio Benavoli, Dario Azzimonti, and Dario Piga. Preferential Bayesian optimization with skew Gaussian processes. In *Proceedings of the Genetic and Evolutionary Computation Conference Companion*, pages 1842–1850, 2021.
- Raul Astudillo and Peter Frazier. Multi-attribute Bayesian optimization with interactive preference learning. In *International Conference on Artificial Intelligence and Statistics*, pages 4496–4507. PMLR, 2020.
- Louis L Thurstone. A law of comparative judgment. In *Scaling*, pages 81–92. Routledge, 2017.
- Daniel Russo and Benjamin Van Roy. Learning to optimize via posterior sampling. *Mathematics of Operations Research*, 39(4):1221–1243, 2014.
- Kirthevasan Kandasamy, Akshay Krishnamurthy, Jeff Schneider, and Barnabás Póczos. Parallelised bayesian optimisation via thompson sampling. In *International Conference on Artificial Intelligence and Statistics*, pages 133–142, 2018.
- Sayak Ray Chowdhury and Aditya Gopalan. On kernelized multi-armed bandits. In Doina Precup and Yee Whye Teh, editors, *Proceedings of the 34th International Conference on Machine Learning*, volume 70 of *Proceedings of Machine Learning Research*, pages 844–853, International Convention Centre, Sydney, Australia, Aug 2017b. PMLR.
- Gene Li, Prithvi Kamath, Dylan J Foster, and Nathan Srebro. Understanding the eluder dimension. In *Advances in Neural Information Processing Systems*, 2021.
- Radford M Neal. *Bayesian learning for neural networks*, volume 118. Springer Science & Business Media, 2012.
- S. Surjanovic and D. Bingham. Virtual library of simulation experiments: Test Functions and Datasets, 2017. URL "<http://www.sfu.ca/~ssurjano>". [Online; accessed 21-January-2023].
- Marc Duquesnoy, Teo Lombardo, Mehdi Chouchane, Emiliano N Primo, and Alejandro A Franco. Data-driven assessment of electrode calendaring process by combining experimental results, in silico mesostructures generation and machine learning. *Journal of Power Sources*, 480:229103, 2020.
- Stavros X Drakopoulos, Azarmidokht Gholamipour-Shirazi, Paul MacDonald, Robert C Parini, Carl D Reynolds, David L Burnett, Ben Pye, Kieran B O'Regan, Guanmei Wang, Thomas M Whitehead, et al. Formulation and manufacturing optimization of Lithium-ion graphite-based electrodes via machine learning. *Cell Reports Physical Science*, 2(12):100683, 2021.
- Nachman Aronszajn. Theory of reproducing kernels. *Transactions of the American mathematical society*, 68(3):337–404, 1950.
- Emilie Kaufmann, Nathaniel Korda, and Rémi Munos. Thompson sampling: An asymptotically optimal finite-time analysis. In *Algorithmic Learning Theory: 23rd International Conference, ALT 2012, Lyon, France, October 29-31, 2012. Proceedings 23*, pages 199–213. Springer, 2012.
- Bobak Shahriari, Ziyu Wang, Matthew W Hoffman, Alexandre Bouchard-Côté, and Nando de Freitas. An entropy search portfolio for Bayesian optimization. *arXiv preprint arXiv:1406.4625*, 2014.
- Hildo Bijl, Thomas B Schön, Jan-Willem van Wingerden, and Michel Verhaegen. A sequential Monte Carlo approach to Thompson sampling for Bayesian optimization. *arXiv preprint arXiv:1604.00169*, 2016.
- Craig L Schmidt and Paul M Skarstad. The future of Lithium and Lithium-ion batteries in implantable medical devices. *Journal of power sources*, 97:742–746, 2001.
- Joel Brunarie, Anne-Marie Billard, Stuart Lansburg, and Mathieu Belle. Lithium-ion (Li-ion) battery technology evolves to serve an extended range of telecom applications. In *2011 IEEE 33rd International Telecommunications Energy Conference (INTELEC)*, pages 1–9. IEEE, 2011.
- Gavin Harper, Roberto Sommerville, Emma Kendrick, Laura Driscoll, Peter Slater, Rustam Stolkin, Allan Walton, Paul Christensen, Oliver Heidrich, Simon Lambert, et al. Recycling Lithium-ion batteries from electric vehicles. *nature*, 575(7781):75–86, 2019.

A Appendix

A.1 Reproducing Kernel Hilbert Spaces

The kernel functions $k(\mathbf{x}, \mathbf{x}') : \mathcal{X} \times \mathcal{X} \rightarrow \mathbb{R}$ used in Gaussian Process (GP) uniquely define an associated Reproducing Kernel Hilbert Space (RKHS) Aronszajn [1950]. Formally:

Definition 3. Let \mathcal{H}_k be a Hilbert space of real valued functions $f : \mathcal{X} \rightarrow \mathbb{R}$ on a non-empty set \mathcal{X} . A function $k : \mathcal{X} \times \mathcal{X} \rightarrow \mathbb{R}$ is a reproducing kernel of \mathcal{H}_k , and \mathcal{H}_k a **Reproducing Kernel Hilbert Space (RKHS)**, if

- $\forall \mathbf{x}, \mathbf{x}' \in \mathcal{X}, k(\mathbf{x}, \mathbf{x}') = \langle k(\cdot, \mathbf{x}), k(\cdot, \mathbf{x}') \rangle_{\mathcal{H}_k}$,
- k spans \mathcal{H}_k i.e., $\forall \mathbf{x} \in \mathcal{X}, k(\cdot, \mathbf{x}) \in \mathcal{H}_k$,
- $\forall \mathbf{x} \in \mathcal{X}, \forall f \in \mathcal{H}_k, \langle f(\cdot), k(\cdot, \mathbf{x}) \rangle_{\mathcal{H}_k} = f(\mathbf{x})$ (the reproducing property).

There exists varieties of kernels that can be used in fitting a GP surrogate model. A kernel that depends only on the distance between two given points i.e., $k = k(\mathbf{x} - \mathbf{x}')$ is called as stationary kernels. Stationary kernels are also called as translation-invariant kernels. Some of the popular kernel functions are listed below.

A.1.1 Matérn Kernel

Matérn kernel is a kernel that is commonly used in numerous machine learning applications. There are two variants of Matérn kernels that differ in their smoothness coefficient (ν) as shown below.

$$k_{\text{MAT}}(\mathbf{x}, \mathbf{x}')_{\nu=\frac{3}{2}} = \left(1 + \frac{\sqrt{3}}{l} \|\mathbf{x} - \mathbf{x}'\|\right) \exp\left(-\frac{\sqrt{3}}{l} \|\mathbf{x} - \mathbf{x}'\|\right) \quad (8)$$

$$k_{\text{MAT}}(\mathbf{x}, \mathbf{x}')_{\nu=\frac{5}{2}} = \left(1 + \frac{\sqrt{5}}{l} \|\mathbf{x} - \mathbf{x}'\| + \frac{\sqrt{5}}{3l^2} \|\mathbf{x} - \mathbf{x}'\|^2\right) \exp\left(-\frac{\sqrt{5}}{l} \|\mathbf{x} - \mathbf{x}'\|\right) \quad (9)$$

where l is the lengthscale hyperparameter of Matérn kernel.

A.1.2 Squared Exponential Kernel

Squared Exponential (SE) kernel or Radial Basis Function (RBF) or Gaussian kernel function is the popular stationary kernel function. The closed-form formulation of the SE kernel is represented as shown below.

$$k_{\text{SE}}(\mathbf{x}, \mathbf{x}') = \sigma_f^2 \exp\left(-\frac{1}{2l^2} \|\mathbf{x} - \mathbf{x}'\|^2\right) \quad (10)$$

where, σ_f^2 and l corresponds to the signal variance and lengthscale hyperparameter, respectively, collectively represented as $\Theta_k = \{l, \sigma_f^2\}$.

A.1.3 Linear Kernel

Linear kernel is a commonly used non-stationary kernels defined as the inner product of the input data points. The mathematical formulation of a linear kernel is given by:

$$k_{\text{LIN}}(\mathbf{x}, \mathbf{x}') = \mathbf{x}' \mathbf{x}^\top + c \quad (11)$$

where c is the bias hyperparameter of linear kernels.

A.1.4 Multi-kernel Learning

Multi-kernel is a non-stationary kernel function defined as a linear combination of stationary and non-stationary kernels. For instance, multi-kernels can be constructed as:

$$k_{\text{MKL}}(\mathbf{x}, \mathbf{x}') = w_1 k_{\text{SE}}(\mathbf{x}, \mathbf{x}') + w_2 k_{\text{MAT}}(\mathbf{x}, \mathbf{x}') + w_3 k_{\text{LIN}}(\mathbf{x}, \mathbf{x}') \quad (12)$$

where $\mathbf{w} = [w_1 \ w_2 \ w_3]$ corresponds to the kernel weights, that are usually tuned by maximizing GP log-likelihood.

A.2 Bayesian Optimization

The central idea of Bayesian Optimization (BO) strategy is to define a prior distribution over all the possible set of objective functions and then refine the model sequentially with the observed samples. BO is built on top of the Bayes theorem that incorporate prior belief about the black-box objective function under consideration. According to Bayes theorem, given a model \mathcal{M} and data \mathcal{D} , the posterior probability of the model conditioned on data *i.e.*, $\mathcal{P}(\mathcal{M}|\mathcal{D})$ is directly proportional to the likelihood of data \mathcal{D} conditioned on model \mathcal{M} *i.e.*, $\mathcal{P}(\mathcal{D}|\mathcal{M})$, multiplied by the prior probability of model $\mathcal{P}(\mathcal{M})$,

$$\mathcal{P}(\mathcal{M}|\mathcal{D}) \propto \mathcal{P}(\mathcal{D}|\mathcal{M}) \mathcal{P}(\mathcal{M}) \quad (13)$$

The observation model of BO is collected as $\mathcal{D}_{1:t} = \{\mathbf{x}_{1:t}, \mathbf{y}_{1:t}\}$, where $y_t = f(\mathbf{x}_t) + \eta_t$ is a noisy observation of the black-box objective function f evaluated at input location \mathbf{x}_t corrupted with a white Gaussian noise $\eta_t \sim \mathcal{GP}(0, \sigma_\eta^2)$. In BO, we compute the posterior distribution $\mathcal{P}(f|\mathcal{D})$ by combining the prior $\mathcal{P}(f)$ with the likelihood $\mathcal{P}(\mathcal{D}|f)$ represented as,

$$\mathcal{P}(f|\mathcal{D}) \propto \mathcal{P}(\mathcal{D}|f) \mathcal{P}(f) \quad (14)$$

The posterior distribution $\mathcal{P}(f|\mathcal{D})$ computed captures our updated belief about the black-box objective function. BO can be perceived as a two step sequential strategy. First step focuses on defining the prior distribution that capture our prior beliefs. Usually GPs are used in placing prior distributions. Second step focuses on determining the best candidate that can be evaluated next. Acquisition functions are used to find the next candidate point with the high promise of finding the optima. An algorithm for the standard Bayesian optimization procedure is provided in Algorithm 2.

Algorithm 2 Standard Bayesian Optimization

Input: Set of observations $\mathcal{D}_{1:t'} = \{\mathbf{x}_{1:t'}, \mathbf{y}_{1:t'}\}$, Sampling budget T

1. **for** $t = t', \dots, T$ iterations **do**
 2. optimize $\Theta^* = \underset{\Theta}{\operatorname{argmax}} \log \mathcal{L}$
 3. update GP model with optimal kernel hyperparameters Θ^*
 4. find the next query point $\mathbf{x}_{t+1} = \underset{\mathbf{x} \in \mathcal{X}}{\operatorname{argmax}} u(\mathbf{x})$
 5. query $f(\mathbf{x})$ at \mathbf{x}_{t+1} as $y_{t+1} = f(\mathbf{x}_{t+1}) + \eta_{t+1}$
 6. augment the data as $\mathcal{D}_{1:t+1} = \mathcal{D}_{1:t} \cup (\mathbf{x}_{t+1}, y_{t+1})$
 7. update GP model
 8. **end for**
-

A.2.1 Acquisition Functions

The acquisition function guides the optimization by balancing the trade-off between exploration and exploitation. Kushner [1964] proposed Expected Improvement (EI) acquisition function to guide the search by taking into account both the probability and magnitude of improvement over the current known optima. The next candidate point is obtained by maximizing the acquisition function given as:

$$u_{\text{EI}}(\mathbf{x}) = \begin{cases} (\mu(\mathbf{x}) - f(\mathbf{x}^+)) \Phi(Z) + \sigma(\mathbf{x}) \phi(Z) & \text{if } \sigma(\mathbf{x}) > 0 \\ 0 & \text{if } \sigma(\mathbf{x}) = 0 \end{cases} \quad (15)$$

$$Z = \frac{\mu(\mathbf{x}) - f(\mathbf{x}^+)}{\sigma(\mathbf{x})}$$

where $\Phi(Z)$ and $\phi(Z)$ represents the Cumulative Distribution Function (CDF) and Probability Distribution Function (PDF) of the standard normal distribution, respectively and $f(\mathbf{x}^+)$ is the best value observed so far in the optimization.

Gaussian Process-Upper Confidence Bound (GP-UCB) acquisition function is another popular acquisition function defined based on confidence bounds criteria. GP-UCB acquisition function is given as:

$$u_{\text{GP-UCB}}(\mathbf{x}) = \mu(\mathbf{x}) + \sqrt{\beta_t} \sigma(\mathbf{x})$$

where β_t is a hyperparameter that balances the exploration-exploitation at iteration t . Srinivas et al. [2012] discussed in detail the possible values for trade-off parameter β_t . Following Brochu et al. [2010], we set the value for trade-off parameter (β_t) at iteration t as:

$$\beta_t = 2 \log \left(\frac{t^{\frac{d}{2}+2}\pi^2}{3\delta'} \right)$$

where $\delta' \in (0, 1)$, d is the number of input dimensions.

A.2.2 Thompson Sampling based Bayesian Optimization

Thompson sampling Thompson [1933] is a randomized selection strategy to select the next candidate for function evaluation by maximizing a random sample drawn from the posterior distribution. There have been significant advancements Kaufmann et al. [2012], Shahriari et al. [2014], Bijl et al. [2016], Chowdhury and Gopalan [2017a] in Thompson sampling literature that demonstrate the theoretical guarantees of Thompson sampling. Russo and Van Roy [2014] provided a Bayesian regret bound for Thompson sampling using the notion of eluder dimension Li et al. [2021]. A complete algorithm of Thompson sampling based Bayesian optimization is provided in Algorithm 3.

Algorithm 3 Thompson Sampling based Bayesian Optimization

Input: Set of observations $\mathcal{D}_{1:t'} = \{\mathbf{x}_{1:t'}, \mathbf{y}_{1:t'}\}$, Sampling budget T

1. **for** $t = t', \dots, T$ iterations **do**
 2. optimize $\Theta^* = \underset{\Theta}{\operatorname{argmax}} \log \mathcal{L}$
 3. update GP model with Θ^*
 4. draw a random sample \mathbf{g}_{t+1} from the updated GP.
 5. find the next query point $\mathbf{x}_{t+1} = \underset{\mathbf{x} \in \mathcal{X}}{\operatorname{argmax}} \mathbf{g}_{t+1}(\mathbf{x})$
 6. query $f(\mathbf{x})$ at \mathbf{x}_{t+1} as $y_{t+1} = f(\mathbf{x}_{t+1}) + \eta_{t+1}$
 7. augment the data as $\mathcal{D}_{1:t+1} = \mathcal{D}_{1:t} \cup (\mathbf{x}_{t+1}, y_{t+1})$
 8. update GP posterior model
 9. **end for**
-

At each iteration $t+1$, Thompson sampling strategy selects a point \mathbf{x}_t that is highly likely to be the optimum according to the posterior distribution i.e., \mathbf{x}_t is drawn from the posterior distribution $\mathcal{P}_{\mathbf{x}^*}(\cdot | \mathcal{D}_{1:t-1})$ conditioned on data $\mathcal{D}_{1:t-1}$. Thompson sampling strategy simplifies if Gaussian Processes (GPs) are used for prior and posterior distributions. For GPs, if \mathbf{g} is a sample drawn from $\mathcal{GP}(\mu_{\mathcal{D}_{1:t-1}}, k_{\mathcal{D}_{1:t-1}})$ we have:

$$\mathcal{P}_{\mathbf{x}^*}(\mathbf{x} | \mathcal{D}_{1:t-1}) = \int \mathcal{P}_{\mathbf{x}^*}(\mathbf{x} | \mathbf{g}) \mathcal{P}(\mathbf{g} | \mathcal{D}_{1:t-1}) d\mathbf{g}$$

The probability $\mathcal{P}_{\mathbf{x}^*}(\mathbf{x} | \mathbf{g})$ has its mass at the maximizer:

$$\underset{\mathbf{x} \in \mathcal{X}}{\operatorname{argmax}} \mathbf{g}(\mathbf{x}) \tag{16}$$

Using this utility, at each iteration $t + 1$, we draw a sample \mathbf{g}_{t+1} from $\mathcal{GP}(\mu_{\mathcal{D}_{1:t-1}}, k_{\mathcal{D}_{1:t-1}})$ and then find its maxima as per Eq. (16). The obtained maxima is used as the next candidate for function evaluation.

A.3 Additional Details of BOAP Framework

As discussed in the main paper, our proposed framework uses a model selection based decision making on whether to choose augmented GP (\mathcal{GP}_h) built on the expert preferential knowledge on abstract properties or the standard GP (\mathcal{GP}_b) for suggesting the next candidate for function evaluation. The arm containing the standard GP model is denoted as Arm-f and the arm containing the augmented GP model is termed as Arm-h. A complete flowchart of our framework is shown in Figure 4.

In BOAP, Arm-f directly models the given objective function $f(\mathbf{x})$, whereas Arm-h models $f(\mathbf{x})$ via a human objective function ($h(\tilde{\mathbf{x}})$) in a search space comprising of inputs that are augmented with the latent abstract properties computed

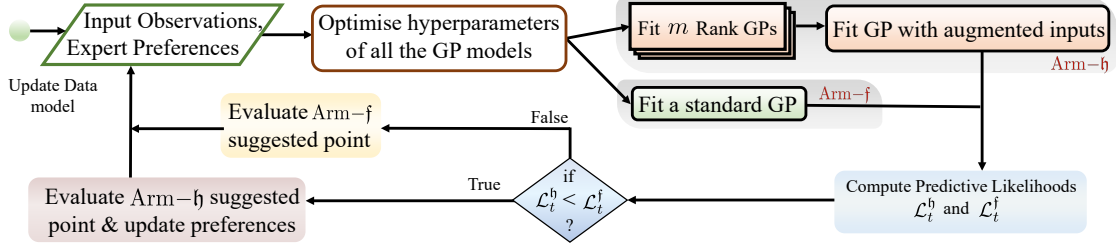


Figure 4: A complete process flowchart of our proposed BOAP framework.

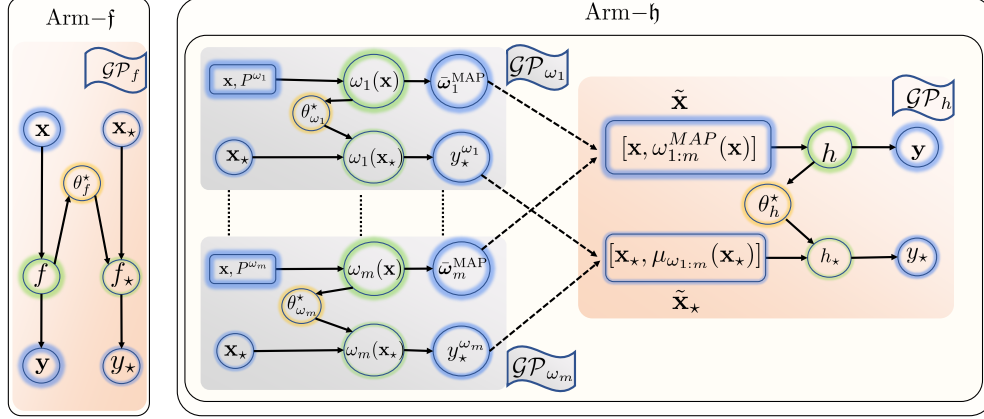


Figure 5: Components of Arm-f and Arm-h in BOAP framework. Nodes highlighted in blue color corresponds to inputs or outputs of a Gaussian process. The estimated parameters and the latent variables are highlighted in yellow and green color, respectively. Rectangular boxes shaded in Grey and Orange correspond to the nodes representing rank GPs and conventional GPs, respectively.

using rank GPs. As discussed in the main paper, the human objective function $h(\tilde{\mathbf{x}})$ incorporates the additional expert feedback from experts, and thus more-informed and a simplified version of $f(\mathbf{x})$. Therefore, at iteration t , if Arm-h is selected and $\tilde{\mathbf{x}}_t = [\mathbf{x}_t, \mu_{\omega_1}(\mathbf{x}_t), \dots, \mu_{\omega_m}(\mathbf{x}_t)]$ is the candidate suggested, then we observe y_t as:

$$y_t = h([\mathbf{x}_t, \mu_{\omega_1}(\mathbf{x}_t), \dots, \mu_{\omega_m}(\mathbf{x}_t)]) \approx f(\mathbf{x}_t)$$

A graphical representation of BOAP framework and its components are shown in Figure 5. Nodes highlighted in blue color corresponds to inputs or outputs of a Gaussian process. Rectangular boxes shaded in Grey correspond to the nodes representing rank GPs, whereas the rectangular boxes shaded in orange correspond to the nodes representing conventional GPs. The estimated parameters and the latent variables are highlighted in yellow and green color, respectively.

A.3.1 Derivatives of the Likelihood Function

In rank GP distributions the MAP estimates are computed using Eq. (4) mentioned in the main paper. However, the Newton-Raphson recursion needs access to the first and second order derivatives of the loss function $L = -\ln \Phi(z(\mathbf{x}, \mathbf{x}'))$ with respect to latent function values ω . The analytical formulation of the first order and second order derivatives are given as:

$$\frac{\partial L}{\partial \omega(\mathbf{x}_i)} = \frac{\Gamma(\mathbf{x}_i) \phi(z)}{\sqrt{2\sigma_\eta^2} \Phi(z)} \quad (17)$$

$$\frac{\partial^2 L}{\partial \omega(\mathbf{x}_i) \partial \omega(\mathbf{x}_j)} = \frac{\Gamma(\mathbf{x}_i) \Gamma(\mathbf{x}_j)}{2\sigma_\eta^2} \left(\frac{\phi^2(z)}{\Phi^2(z)} + z \frac{\phi(z)}{\Phi(z)} \right) \quad (18)$$

$$\text{where } \Gamma_{(\mathbf{x}, \mathbf{x}')}(\mathbf{x}_i) = \begin{cases} 1 & \text{if } \mathbf{x} = \mathbf{x}_i \\ -1 & \text{if } \mathbf{x}' = \mathbf{x}_i \\ 0 & \text{Otherwise} \end{cases}$$

A.4 Additional Results and Experimental Details

A.4.1 Parameter Selection in BOAP framework

The kernel functions (k) used in fitting a Gaussian process model for the unknown objective function f is associated with its own hyperparameter set θ . The optimal kernel hyperparameters (θ^*) are estimated by maximizing the marginal likelihood function, given by the equation:

$$\mathcal{P}(\mathbf{y}|\mathbf{X}, \theta) = \int p(\mathbf{y}|f) p(f|\mathbf{X}, \theta) df \quad (19)$$

By marginalizing Eq. (19), we get the closed-form for GP log-likelihood as:

$$\mathcal{L} = \log \mathcal{P}(\mathbf{y}|\mathbf{X}, \theta) = -\frac{1}{2}(\mathbf{y}^\top [\mathbf{K} + \sigma_\eta^2 \mathbf{I}]^{-1} \mathbf{y}) - \frac{1}{2} \log |\mathbf{K} + \sigma_\eta^2 \mathbf{I}| - \frac{n}{2} \log(2\pi) \quad (20)$$

where n corresponds to the total number of training instances. For a rank GP the closed-form of the GP log-likelihood can be obtained as:

$$\bar{\mathcal{L}} = -\frac{1}{2} \boldsymbol{\omega}_{\text{MAP}}^\top [\mathbf{K} + \sigma_\eta^2 \mathbf{I}]^{-1} \boldsymbol{\omega}_{\text{MAP}} - \frac{1}{2} \log |\mathbf{K} + \sigma_\eta^2 \mathbf{I}| - \frac{n}{2} \log(2\pi) \quad (21)$$

The only difference in the formulation of log-likelihood of a rank GP and a traditional GP is that the absolute measurements (\mathbf{y}) of the objective function is replaced with the latent function values obtained via Maximum A Posteriori (MAP) estimates. The GP log-likelihood mentioned in Eq. (20) and Eq. (21) is now maximized to find the optimal hyperparameters θ^* .

$$\theta^* = \underset{\theta}{\operatorname{argmax}} \mathcal{L}$$

Further, if we use all training instances for the computation of the log marginal likelihood, there are chances that only Control arm may get selected in majority of the rounds. Therefore to avoid this, instead of using all the training instances for computing the marginal likelihood, we use only the subset of the original training data for finding the optimal hyperparameter set and then we use the held-out instances from the original training set to compute the (predictive) likelihood.

In this paper, we implement Automatic Relevance Determination (ARD) kernel Neal [2012] based on Squared Exponential kernel mentioned in Eq. (10) at all levels of our proposed BOAP framework. ARD kernel is popular in the machine learning community due to its ability to suppress the irrelevant features. In ARD, each input dimension is assigned a different lengthscale parameter to keep track of the relevance of that dimension. Therefore, a GP fitted in a d -dimensional input space with ARD kernel has d lengthscale parameters *i.e.*, $\mathbf{l} = l_{1:d}$ and optional variance hyperparameters (noise variance σ_η^2 and signal variance σ_f^2).

Specifically, for the human-inspired arm (Arm-h) we use a spatially-varying ARD kernel where we set the lengthscales of the augmented input dimensions in proportion to the rank GP uncertainties via a parametric function of the input \mathbf{x} . The lengthscale function for each of the augmented input dimension (corresponding to property ω_i) is set to be $l_{\omega_i}(\mathbf{x}) = \alpha \sigma_{\omega_i}(\mathbf{x})$, where α is the scale parameter and $\sigma_{\omega_i}(\mathbf{x})$ is the normalized standard deviation predicted using the rank GP (\mathcal{GP}_{ω_i}). Therefore, the hyperparameter set (θ_h) of Arm-h consists of the lengthscale parameters ($l_{1:D}$) for the original un-augmented dimensions and the scale factor (α) from the augmented input dimensions *i.e.*, $\theta_h = \{l_{1:D}, \alpha\}$.

The overall hyperparameter set Θ of our proposed framework consists of hyperparameters from each of the m rank GPs ($\theta_{\omega_{1:m}}$) and two main GPs corresponding to the 2-arms (θ_h and θ_f) *i.e.*, $\Theta = \{\theta_h, \theta_f\} = \{\{l_{1:D}, \alpha\}, \{l_{1:D}\}\}$. At each iteration t , we find the optimal set of hyperparameters $\Theta_t^* = \{\theta_h^*, \theta_f^*\}$ by maximizing the GP (predictive) log-likelihood mentioned in Eq. (20) and Eq. (21).

In all our experiments, we set the signal variance parameter $\sigma_f^2 = 1$ as we standardize the outputs of \mathcal{GP}_h and \mathcal{GP}_f . We set the noise variance as $\eta \sim \mathcal{GP}(0, \sigma_\eta^2 = 0.1)$ and $\tilde{\sigma}_\eta^2 = 0.1$. As we normalize the input space of the GP distributions

constructed in our BOAP framework, we tune each lengthscale hyperparameter $l \in \Theta$ in the interval $[0, 1]$. Further, we normalize the outputs of each of the auxiliary rank GPs (\mathcal{GP}_{ω_i}) to avoid different scaling levels in their output, that can lead to undesired structures in the augmented input space.

We run all our experiments on an Intel Xeon CPU@ 3.60GHz workstation with 16 GB of RAM capacity. We repeat our experiments with 10 different random initialization. For a d -dimensional problem, we consider $t' = d + 3$ initial observations. The evaluation budget is set as $T = 10 \times d + 5$. For the real-world battery design experiments, due to their expensive nature, we have restricted the evaluation budget to 50 iterations even though $d \gg 5$. In all our experiments, we start with $p = \binom{t'}{2}$ preferences in P , that gets updated in every iteration of the optimization process.

A.4.2 Ablation Studies of BOAP Framework

To demonstrate the robustness of our approach we have conducted additional experiments by accounting for the inaccuracy or poor choices in expert preferential knowledge. Here, we show the performance of our BOAP approach in two scenarios. First, we show the performance of our proposed approach when the higher-order abstract properties are poorly selected. Second, we incorporate noise in the expert preferential feedback by flipping the expert preference between two inputs (designs) with probability $\delta = 0.3$. We now discuss in detail the aforementioned two variations of our proposed method.

Inaccurate Abstract Properties (BOAP-IA) In the first variation, we assume that the expert poorly selects the human abstraction features. Table 2 depicts the synthetic functions considered and the corresponding (poorly chosen) human abstraction features. BOAP-IA uses such inaccurate human abstract features while augmenting the original input space.

Table 2: Selection of abstraction features by a simulated human expert. The human abstraction (high level) features shown in the 3rd column are deliberately selected to be uninformative.

Functions	$f(\mathbf{x})$	Human Abstraction Features
Benchmark	$\exp^{(2-\mathbf{x})^2} + \exp^{\frac{(6-\mathbf{x})^2}{10}} + \frac{1}{\mathbf{x}^2+1}$	$\omega_1 = \sin \mathbf{x}, \omega_2 = \cos \mathbf{x}$
Rosenbrock	$\sum_{i=1}^{d-1} [100 \times (x_{i+1} - x_i^2)^2 + (x_i - 1)^2]$	$\omega_1 = \sin \mathbf{x}, \omega_2 = \cos \mathbf{x}$
Griewank	$\sum_{i=1}^d \left[\frac{x_i^2}{4000} - \prod_{i=1}^d \cos\left(\frac{x_i}{\sqrt{i}}\right) + 1 \right]$	$\omega_1 = \sin \mathbf{x}, \omega_2 = \mathbf{x}^3$

Noisy Expert Preferences (BOAP-NP) In the second variation, we account for the inaccurate expert preferential knowledge by introducing an error in human expert preferential feedback. To do this, we flip the preference ordering with a probability δ (we used $\delta = 0.3$) i.e., $P^{\omega, \delta} = \{(\mathbf{x}_i \succ \mathbf{x}_j) \mid \mathbf{x}_i, \mathbf{x}_j \in \mathbf{x}_{1:n}, \nu_{ij} \omega(\mathbf{x}_i) > \nu_{ij} \omega(\mathbf{x}_j)\}$, where ν_{ij} is drawn from a random distribution such that it is $+1$ with probability $1 - \delta$, -1 with probability δ .

We evaluate the performance by computing the simple regret after $10d$ iterations. The experimental settings are retained as mentioned in the experiments section (refer to Section 5.1 in the main paper). The empirical results for BOAP with inaccurate features (BOAP-IA) and BOAP framework with noisy preferences (BOAP-NP) are presented in Figure 6. It is significant from the results that our proposed BOAP framework outperforms standard baselines due to the model selection based 2-arm scheme employed that intelligently chooses the arm with maximum predictive likelihood to suggest the next sample.

A.4.3 Details of Real-world Experiments

As mentioned in the main paper, we evaluate the performance of BOAP framework in two real-world optimization paradigms in the Lithium-ion battery manufacturing. The advent of cheap Li-ion battery technology has significantly transformed range of industries including healthcare Schmidt and Skarstad [2001], telecommunication Brunarie et al. [2011], automobiles Harper et al. [2019], and many more due to its ability to efficiently store the electrochemical energy. However, the process for manufacturing of Li-ion batteries is very complex and expensive in nature. Thus, there is a wide scope for optimizing the battery manufacturing process to reduce its CapEx and OpEx. We now provide a brief discussion on battery manufacturing experiments considered in our main paper. For real-world experiments, we use the same set of algorithmic parameters that we used in the synthetic experiments.

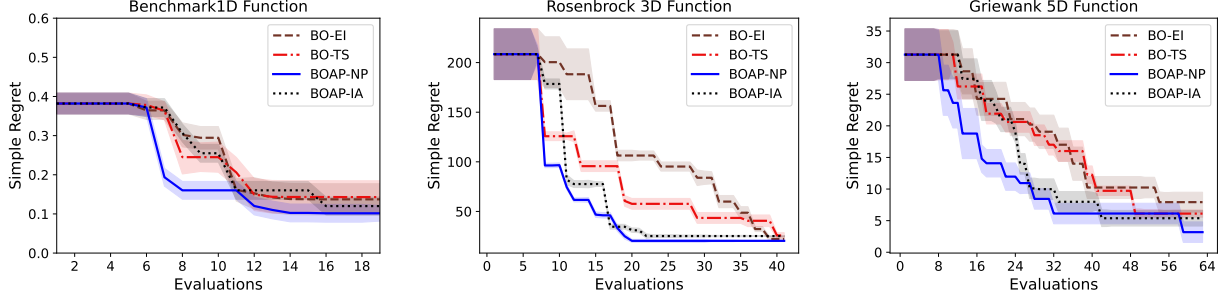


Figure 6: Simple regret vs iterations for the synthetic multi-dimensional benchmark functions. We plot the average regret along with its standard error obtained after 10 random repeated runs.

Optimization of Electrode Calendering Process

Duquesnoy et al. [2020] discussed the effect of calendering process on electrode properties that significantly contribute to the underlying electrochemical performance of a battery. Authors have implemented a data-driven stochastic electrode structure generator, based on which they construct electrodes and analyze in terms of *Tortuosity* (both in solid phase τ_{sol} and liquid phase τ_{liq}), percentage of *Current Collector* (CC) surface covered by the active material and percentage of *Active Surface* (AS) covered by the electrolyte. The manufacturing process parameters considered are calendering pressure, Carbon-Binder Domain (CBD), initial electrode porosity and electrode composition. A pictorial representation of the inter dependencies between the input process variables and output electrode properties is provided in Figure 8 of Duquesnoy et al. [2020].

Duquesnoy et al. [2020] published a dataset reporting the input manufacturing process parameters and the output characteristics of 8800 electrode structures. Each of the manufacturing setting has been evaluated for 10 times, therefore we have averaged the results to obtain a refined dataset consisting of $n = 880$ instances with $d = 8$ process variables.

We optimize the calendering process by maximizing the *Active Surface* of an electrode (overall objective) by modeling two abstract properties: (i) Property 1 (ω_1): *Tortuosity in liquid phase* τ_{liq} , and (ii) Property 2 (ω_2): *Output Porosity* (OP). As discussed in the main paper, the abstract properties $\{\omega_{\tau_{\text{liq}}}, \omega_{\text{OP}}\}$ can only be qualitatively measured, however to simulate the expert pairwise preferential inputs $\{P^{\omega_{\tau_{\text{liq}}}}, P^{\omega_{\text{OP}}}\}$, we use the empirical measurements for τ_{liq} and OP in the published dataset.

$$P^{\omega_{\tau_{\text{liq}}}} = \{(\mathbf{x} \succ \mathbf{x}')_i \mid \tau_{\text{liq}}(\mathbf{x}) > \tau_{\text{liq}}(\mathbf{x}') \mid \mathbf{x}, \mathbf{x}' \in \mathbf{x}_{1:n} \quad \forall i \in \mathbb{N}_p\}$$

$$P^{\omega_{\text{OP}}} = \{(\mathbf{x} \succ \mathbf{x}')_i \mid \text{OP}(\mathbf{x}) > \text{OP}(\mathbf{x}') \mid \mathbf{x}, \mathbf{x}' \in \mathbf{x}_{1:n} \quad \forall i \in \mathbb{N}_p\}$$

We obtain the values $\tau_{\text{liq}}(\mathbf{x})$ and $\text{OP}(\mathbf{x})$ by referring to the dataset published. Based on these preference lists $\{P^{\omega_{\tau_{\text{liq}}}}, P^{\omega_{\text{OP}}}\}$, we fit two auxiliary rank GP distributions $\{\mathcal{GP}_{\omega_{\tau_{\text{liq}}}}, \mathcal{GP}_{\omega_{\text{OP}}}\}$. Then, we use these auxiliary rank GPs to augment the input space of the main GP surrogate \mathcal{GP}_h modeling the overall objective i.e., active surface of the electrode.

Optimization of Electrode Manufacturing Process

In a similar case study Drakopoulos et al. [2021], the authors have analyzed the manufacturing of Lithium-ion graphite based electrodes. The main aim of Drakopoulos et al. [2021] is to optimize the formulation and manufacturing process of Lithium-ion electrodes using machine learning. Authors have established a relationship between the process parameters at different stages of manufacturing such as mixing, coating, drying, and calendering. The published dataset records all the process parameters in manufacturing 256 coin cells, as well as the associated results showing the charge capacity of each coin cell measured after certain charge-discharge cycles. The refined dataset consists of 12 process variables, out of which two process variables: (i) *Anode Thickness* (AT), and (ii) *Active Mass* (AM) are treated as abstract properties that can be only qualitatively measured. The overall objective here is to maximize the battery endurance $E = \frac{D_{50}}{D_5}$, where D_{50} and D_5 are the discharge capacities of the cell at 50th cycle and 5th cycle, respectively.

We simulate the expert pairwise preferential inputs $\{P^{\omega_{\text{AT}}}, P^{\omega_{\text{AM}}}\}$ by comparing the empirical values recorded for these variables in the given dataset.

$$P^{\omega_{\text{AT}}} = \{(\mathbf{x} \succ \mathbf{x}')_i \mid \text{AT}(\mathbf{x}) > \text{AT}(\mathbf{x}') \mid \mathbf{x}, \mathbf{x}' \in \mathbf{x}_{1:n} \quad \forall i \in \mathbb{N}_p\}$$

$$P^{\omega_{\text{AM}}} = \{(\mathbf{x} \succ \mathbf{x}')_i \text{ if } \text{AM}(\mathbf{x}) > \text{AM}(\mathbf{x}') \mid \mathbf{x}, \mathbf{x}' \in \mathbf{x}_{1:n} \quad \forall i \in \mathbb{N}_p\}$$

We model abstract properties $\{\omega_{\text{AT}}, \omega_{\text{AM}}\}$ by fitting rank GPs $\{\mathcal{GP}_{\omega_{\text{AM}}}, \mathcal{GP}_{\omega_{\text{AT}}}\}$ using preference lists $\{P^{\omega_{\text{AM}}}, P^{\omega_{\text{AT}}}\}$. We use rank GPs to estimate the abstract properties and then use those estimations to augment the input space of the main GP modeling the overall objective i.e., maximizing battery endurance E .

A.5 Limitations

Firstly, as discussed in Convergence Remarks section in the main paper, if the expert preferential data is inaccurate or irrelevant, it may mislead the model and increase eluder dimension, thus impeding convergence. Although the ablation studies show the robustness of BOAP against inaccurate/noisy expert preferences, our framework may suffer at least in the initial rounds of the optimization until the Control arm identifies and dominates to suppress the inaccurate/noisy human-inspired model (Arm-h). Secondly, BOAP in its vanilla version may not be directly scalable because of the scalability issues of the underlying range of GPs used in the framework. One of the well-known weaknesses of GP is that it poorly scales and suffers from a cubic time complexity $O(n^3)$ due to the inversion of the gram matrix \mathbf{K} . This limits the scalability of GP and thus our BOAP framework to use with large-scale datasets. In the future line of work, we aspire to overcome these limitations by employing suitable GP techniques that can be easily scaled.